Tensile properties of helical auxetic structures: A numerical study

J. R. Wright,[a] M. R. Sloan, and K. E. Evans
School of Engineering, Mathematics and Physical Sciences, University of Exeter, North Park Road, Exeter EX4 4QF, United Kingdom

(Received 11 March 2010; accepted 16 June 2010; published online 18 August 2010)

This paper discusses a helical auxetic structure which has a diverse range of practical applications. The mechanical properties of the system can be determined by particular combinations of geometry and component material properties; finite element analysis is used to investigate the static behavior of these structures under tension. Modeling criteria are determined and design issues are discussed. A description of the different strain-dependent mechanical phases is provided. It is shown that the stiffnesses of the component fibers and the initial helical wrap angle are critical design parameters, and that strain-dependent changes in cross-section must be taken into consideration: we observe that the structures exhibit nonlinear behavior due to nonzero component Poisson's ratios. Negative Poisson's ratios for the helical structures as low as −5 are shown. While we focus here on the structure as a yarn our findings are, in principle, scaleable. © *2010 American Institute of Physics*. [doi:10.1063/1.3465378]

I. INTRODUCTION

An auxetic material is one which exhibits a negative Poisson's ratio.[1] Many examples, both synthetic and naturally occurring, have been investigated during the last 20 years, including the production of polymeric foams with reentrant auxetic cells by cycles of heating and mechanical deflection;[2,3] honeycomb structures;[4] microstructural changes in polyethylene induced by sintering;[5] skin[6] and rotation of molecular bonds in zeolites,[7] and single crystal arsenic.[8]

One of the most promising auxetic mechanisms for practical exploitation is the helical auxetic yarn (HAY), first reported by Hook in 2003.[9] This structure has applications in composites and in textiles, and is under development for applications as diverse as healthcare,[10] safety restraints, body armour,[11] blast mitigation, and filtration.[12]

The HAY is a fiber structure comprised of two components, one component being the *core* around which is helically wound the second, *wrap*, fiber (Fig. 1). Under tension the wrap tends to straighten, thereby causing the core to displace laterally in a helical manner (Fig. 2). If the wrap fiber is of a lower diameter than the core this behavior can result in a nett increase in the effective diameter of the composite yarn—a negative Poisson's ratio. Such behavior opens up a wealth of interesting possible textile applications based around exploiting the ability to cause pores to open (Fig. 3).

Miller *et al.*[13] have conducted an experimental study of a composite including a textile with HAYs in the weft. At some intermediate strain both components take on a helical form, and Miller *et al.* describe the HAY as a "double helix yarn"; under certain design conditions it is possible that the structure will not exhibit auxetic behavior[14] and it is a purpose of this paper to explore the behavior of the yarn and to determine conditions under which it will indeed be auxetic.

Yarn modeling has been the subject of much attention over many decades, primarily focused on behavior when incorporated in textiles. Ramgulam and Potluri[15] derive a model for an elastica combining geometrical and mechanical properties and apply this to a multifilament yarn consisting of layers of helical fibers; promising agreement with experimental data is indicated. However, this model is intended for (lateral) compression modeling of the yarn and the filaments are assumed to be inextensible. Batra[16] examined lateral pressures between individual filaments in a multifilament yarn by considering a helical fiber wound around a cylinder to model the effects of interfilament forces during manufacture and processing of twisted yarns. Phillips and Costello[17] calculated an "effective modulus" for a complex wire rope by analyzing the deformation of a helical filament in a straight strand of rope. Ghoreishi *et al.*[18] developed an analytical model for a yarn comprised of six helical strands around a central core. Transverse displacements were not considered. Hearle and Konopasek[19] give a comprehensive summary of alternative approaches to analytical modeling of twisted yarns (being continuous helical multifilament structures) and consider the effect of Poisson's ratio of individual filaments. All of these works (and numerous others cited within) concentrate of necessity on conventional yarn structures and therefore do not consider the effects of only one helical fiber upon a cylindrical core.

Numerical techniques have been used to analyze behavior of other auxetic structures. Lira *et al.*[20] used a finite element (FE) model to validate an analytical model for shear in auxetic honeycombs, showing agreement generally within

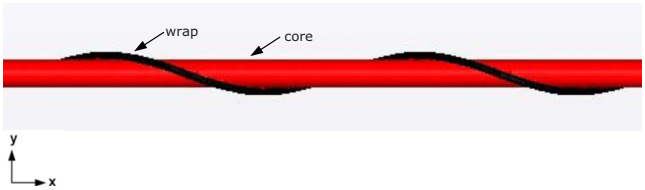

FIG. 1. (Color online) Components of the HAY.

[a]Electronic mail: j.r.wright@exeter.ac.uk.

FIG. 2. (Color online) Auxetic behavior under tension.

3%. Their approach was to model a *representative volume element*, or "unit cell" with appropriate boundary conditions.

This paper defines the geometry of the HAY and reports the results of numerical modeling using finite element analysis (FEA) to evaluate the tensile design envelope of HAYs having low-modulus elastomeric cores, discussing in particular the effects of nonlinear behavior in the component fibers and the effects of cross-sectional changes upon yarn performance. We focus here on an elastomeric core and monofilament components.

II. TERMINOLOGY AND DEFINITIONS

This paper will discuss important distinctions between the *engineering* and *true*, and *longitudinal* and *lateral*, values of stress, strain, and tensile modulus. For clarity, true and lateral values are indicated explicitly. Where there is no indication, values may be taken to be engineering and/or longitudinal. For example, "strain" refers to longitudinal engineering strain.

Figure 4 shows one complete cycle of the HAY. We define the nominal wrap angle θ as the angle subtended by the axis of the core and the axis of the wrap at zero strain. The longitudinal distance for one complete cycle is termed the pitch, λ. Pitch may be determined more readily than wrap angle, although the latter is intuitively preferred as a defining parameter of the yarn. The diameters of the unstrained core and wrap are D_c and D_w, respectively.

If we take exactly one cycle of HAY and roll it out vertically such that the wrap "unwraps and sticks to the paper" we form a right triangle as per the larger of the two in Fig. 5 below. However, this gives (on the hypotenuse) a measure of the developed length (L_w') of the outermost edge of the wrap; the actual wrap length L_w is given by the locus of the center of the wrap helix. The latter is determined by the circumferential distance $\pi(D_c+D_w)$. For a given combination of λ and θ we may prescribe the sum (D_c+D_w), i.e., there is a range of available D_c/D_w. More typically we will prescribe θ for a given combination of D_c and D_w and this will determine λ, thus allowing manufacture by specification of λ.

From Fig. 5 we obtain

$$\tan\theta = \pi(D_c + D_w)/\lambda, \tag{1}$$

$$L_w = \sqrt{[\pi^2(D_c + D_w)^2 + \lambda^2]}, \tag{2}$$

FIG. 3. (Color online) Textile application—pores open under tension in a complementary pair of HAYs.

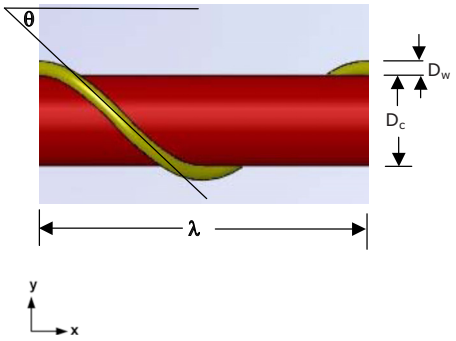

FIG. 4. (Color online) Geometry of the HAY.

$$\lambda = L_w \cos\theta. \tag{3}$$

Poisson's ratio is defined as the ratio of lateral contractile strain (ε_y) to longitudinal tensile strain (ε_x) for a material under longitudinal tension

$$\nu = -\varepsilon_y/\varepsilon_x. \tag{4}$$

We define the *effective diameter*, D_e, of the HAY as the diameter of a cylinder which would precisely contain the yarn at any given strain; this is the dimension which will normally be exploited in practical applications of the technology. Then the Poisson's ratio of the HAY is given by

$$\nu = -\frac{(D_e - D_{eo})/D_{eo}}{(L - L_o)/L_o}, \tag{5}$$

where D_{eo} is the effective diameter of the HAY at zero strain $(=D_c+2D_w)$, L is the length of the HAY, and L_o is the length of the HAY at zero strain.

III. METHOD

Modeling was carried out using the commercial software ABAQUS V6.8–3.[21] The solver used was the Abaqus/Standard Full-Newton Iteration symmetric solver. All computations were carried out on a 3 GHz Xeon 5450 with 18 GB RAM, and all models used 10-noded quadratic tetrahedral elements (Abaqus element C3D10M) and default Abaqus convergence tolerances (Table I). Input geometry for the FE Analysis was generated from parametric SolidWorks[22] models, greatly increasing the efficacy of model generation.

The tensile test is simulated by encastring (restricting all six translational and rotational degrees of freedom) all nodes on the surfaces at one end of the test specimen. The other end is subjected to a prescribed displacement only in the

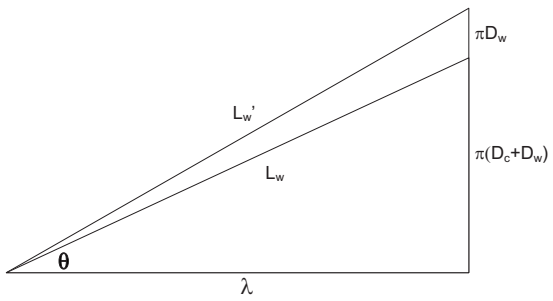

FIG. 5. "Unwrapped" geometry of the HAY.

TABLE I. Default Abaqus convergence criteria used in all models.

Criterion for residual force for a nonlinear problem	5.00×10^{-3}
Criterion for displacement correction in a nonlinear problem	1.00×10^{-2}
Initial value of time average force	1.00×10^{-2}
Average force is time average force	
Alternate criterion for residual force for a nonlinear problem	2.00×10^{-2}
Criterion for zero force relative to time average force	1.00×10^{-5}
Criterion for residual force when there is zero flux	1.00×10^{-5}
Criterion for displacement correction when there is zero flux	1.00×10^{-3}
Criterion for residual force for a linear increment	1.00×10^{-8}
Field conversion ratio	1
Criterion for zero force relative to time average maximum force	1.00×10^{-5}
Criterion for zero displacement relative to characteristic length	1.00×10^{-8}

axial direction and is restrained from translation in the other two directions. A precise determination of the practical boundary conditions is a research topic in its own right: the issues are discussed by Sloan *et al.*[14] A sum of the resultant axial reaction forces on the displaced end surface(s) is then taken as the total reaction force.

Tensile modulus E is the ratio of stress (σ) to strain (ε)

$$\mathrm{E} = \sigma/\varepsilon, \tag{6}$$

stress being the ratio of force (F) to cross-sectional area (A) and strain the ratio of change in length (ΔL) to original length (L)

$$\sigma = \mathrm{F/A}, \tag{7}$$

$$\varepsilon = \Delta\mathrm{L/L}, \tag{8}$$

from which we obtain

$$\mathrm{E} = \mathrm{FL/A}\ \Delta\mathrm{L}. \tag{9}$$

Thus from a computation of reaction force F for a given displacement ΔL and measurement of cross-sectional area A we can derive tensile modulus E. If we assume A does not change we derive engineering tensile modulus; if we measure changes in A to obtain true stress and calculate true strain ε_T from

$$\varepsilon_\mathrm{T} = \ln(1+\varepsilon), \tag{10}$$

we obtain true tensile modulus.

Cross-sectional areas were measured by acquiring screenshot images of yarn sections and processing these using the IMAGEJ[23] public domain image processing software with appropriate calibration.

Lateral strains and hence Poisson's ratios were obtained by calculating the nodal displacements and displaying the lateral (in this case, y-axis) components (Fig. 6). Maximum and minimum values were then recorded to give effective diameter and thereby Poisson's ratio.

For all models the contact condition between core and wrap is a tie constraint, i.e., assuming to a first approximation that there is perfect contact-no slip or friction condition.

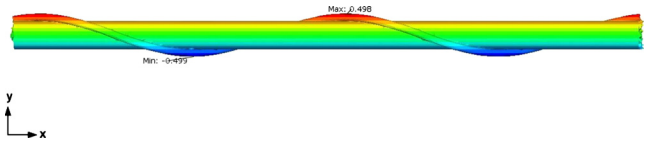

FIG. 6. (Color online) Measurement of effective diameter from maximum and minimum lateral nodal displacements.

The following study first establishes the accuracy of the FEA tool and then proceeds to examine the effect of several design parameters upon HAY performance, viz, core/wrap diameter ratio; wrap angle; component and yarn tensile moduli; component and yarn Poisson's ratios.

IV. RESULTS AND DISCUSSION

The HAY models discussed in Secs. IV A–IV C are for a 648.5 μm (600 μm nominal) diameter polyurethane core, engineering tensile modulus (E)=150 MPa and Poisson's ratio (ν)=0.45, and 97.4 μm (100 μm nominal, "wrap A") and 174.5 μm (150 μm nominal, "wrap B") diameter polyamide wraps, E=10 GPa and ν=0.45; see Table II for a summary. The data are taken from indicative tensile tests and from Scanning Electron Microscope (SEM) measurements.

Section IV D discusses the effect of changing the tensile modulus of the wrap; Sec. IV E compares engineering and true tensile moduli; Sec. IV F examines the effect of changing Poisson's ratios of the yarn components, and Sec. IV G discusses the auxetic behavior of the HAY.

A. Model accuracy

Model accuracy was checked using a HAY with wrap B and θ=20°.

1. End effects

The choice of boundary conditions will have localized effects on the yarn behavior, so it is necessary to establish how many wrap cycles should be modeled in order that end effects will have negligible influence upon measurements in the central region of the yarn. Figure 7 shows the effect of wrap cycle count upon predicted reaction force in the HAY. Results for the 10-cycle model lie within 1.5% of the 50-cycle model, and therefore 10-cycle model is considered acceptable for the remaining models. For the purpose of effective diameters, lateral strains and Poisson's ratios, maximum dimensions were derived only from the central 2 cycles of each model.

TABLE II. Typical component properties for the majority of the models.

Component	Material	Diameter (μm)	Tensile modulus (MPa)	Poisson's ratio
Core	Polyurethane	648.5	150	0.45
Wrap A	Polyamide	97.4	10 000	0.45
Wrap B	Polyamide	174.5	10 000	0.45

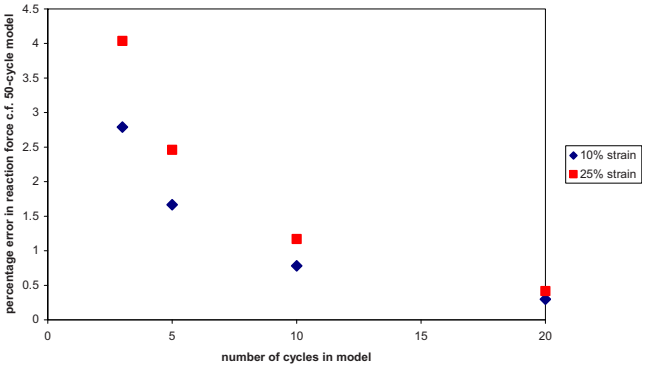

FIG. 7. (Color online) Effect of cycle count on reaction force in yarn, evaluated at 3, 5, 10, and 20 cycles and each compared to a 50-cycle model.

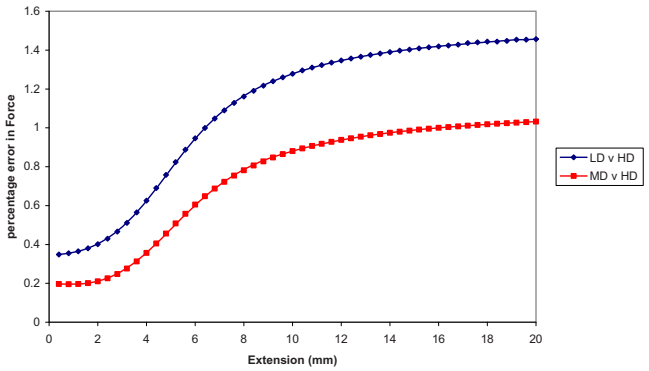

FIG. 8. (Color online) Effect of mesh density upon predicted yarn reaction force, comparing accuracy of LD vs HD and MD vs HD meshes.

2. Effect of mesh density

Three mesh densities were evaluated. Table III reports the mesh parameters.

Figure 8 shows the effect of mesh density upon predicted behavior of the yarn; 20 mm extension corresponds to approximately 30% strain (initial model length=71.037 mm). Accuracy deteriorates at higher strains due to element distortion; however, the medium density (MD) mesh results lie within approximately 1% of the results for the high density (HD) mesh (red curve), while solving some 2.5 times faster. Based on this data a typical element dimension of 0.1 mm was used in the ensuing analyses.

B. Core/wrap diameter ratio

An important property of the HAY is the ratio of core diameter to wrap diameter. Although the tensile moduli of the core and wrap materials differ by nearly two orders of magnitude, the *stiffnesses* of the fiber structures are the key influence on yarn performance.

Stiffness K, being the ratio of force to extension, is related to modulus from Eq. (9) by

$$K = EA/L. \tag{11}$$

Thus the stiffness of the fibers is directly dependent upon A and therefore fiber diameter.

Figure 9 shows the force versus extension data for the core and the two wraps and corresponding stiffnesses are shown in Fig. 10, showing that wrap A is unlikely to be fit for purpose because it is less than twice as stiff as the core. The behavior is inherently nonlinear due to the finite component Poisson's ratios: as a result the component cross-sectional areas reduce with increasing strain.

C. Wrap angle

Perhaps the most significant design variable, given likely commercial constraints upon choice of components, is the choice of wrap angle. Figure 11 shows the effect of wrap angle upon (engineering) tensile modulus for the yarn using wrap B, and Fig. 12 compares the performance of the two wraps for $\theta=20°$.

The yarn with wrap A exhibits significantly lower maximum tensile modulus in accordance with the observations of Sec. IV B. The initial (zero-strain) composite modulus tends asymptotically toward the modulus of the core (150 MPa). The lower the wrap angle, the more rapid the increase in gradient of the modulus. For medium angles the analysis does not converge at higher strains due to the combination of high rate of change in the stiffness matrix and increasing element distortion.

The change in yarn modulus is caused by the competition between two mechanisms–the wrap is tending to straighten and simultaneously inducing lateral displacement in the core. At low strains the modulus is dominated by the core, but as the wrap straightens and itself becomes strained the yarn modulus is influenced by stress in the wrap.

At higher wrap angles the presence of the wrap is not significant even at 30%–40% strain. This is explained by Fig. 13, which compares the change in effective diameter of a 20° self-supporting helix (i.e., a spring) with that of a 60°

TABLE III. Parameters for mesh convergence study. "Typical element dimension" is the Abaqus "approximate global size" parameter which controls mesh seeding. "Mesh density" is the ratio of number of elements to model volume.

Mesh quality	Typical element dimension (mm)	Number of elements in mesh	Model volume (mm^3)	Mesh density (elements/mm^3)	Computation time (min./data point)
Low (LD)	0.125	131 461	25.27	5202	6.1
MD	0.100	246 700	25.27	9763	13.9
HD	0.075	400 230	25.27	15 838	34.4

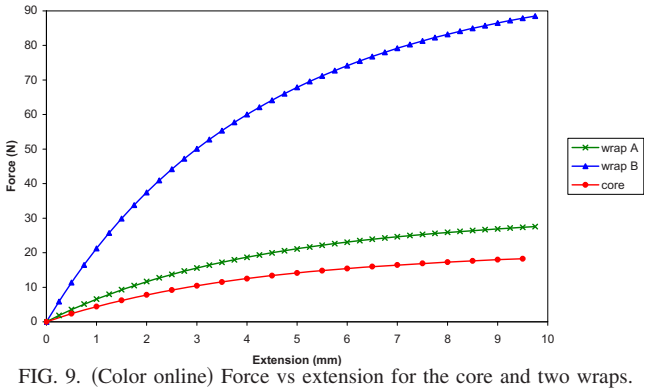

FIG. 9. (Color online) Force vs extension for the core and two wraps.

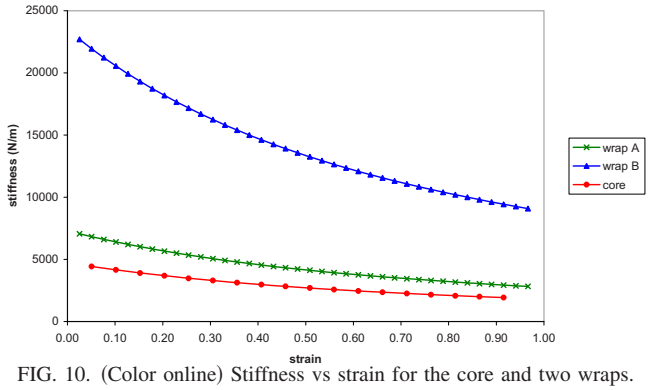

FIG. 10. (Color online) Stiffness vs strain for the core and two wraps.

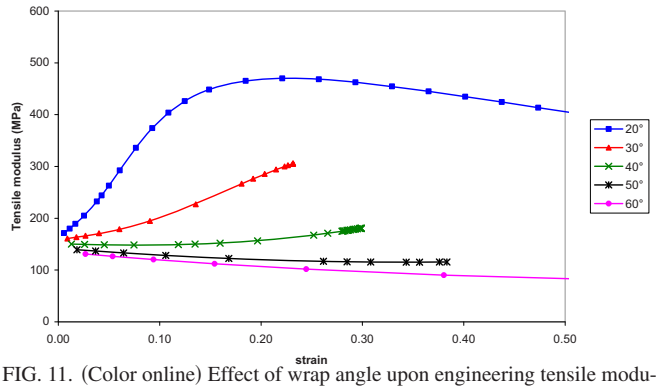

FIG. 11. (Color online) Effect of wrap angle upon engineering tensile modulus of yarn with wrap B.

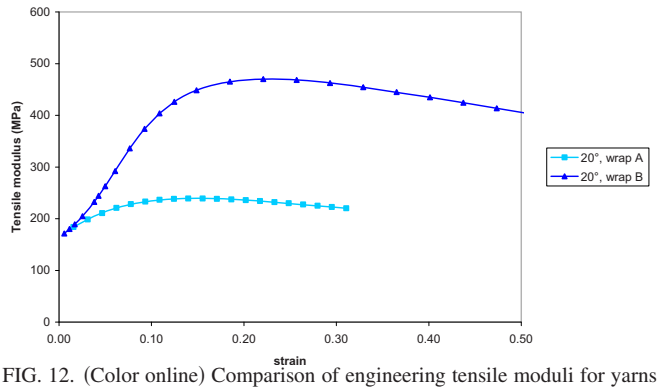

FIG. 12. (Color online) Comparison of engineering tensile moduli for yarns with wrap A and wrap B at $\theta=20°$.

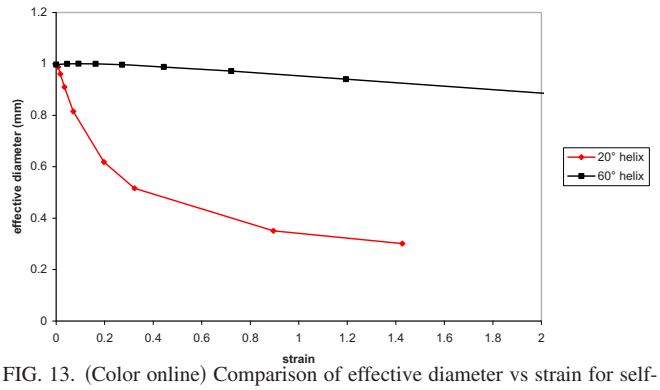

FIG. 13. (Color online) Comparison of effective diameter vs strain for self-supporting helices.

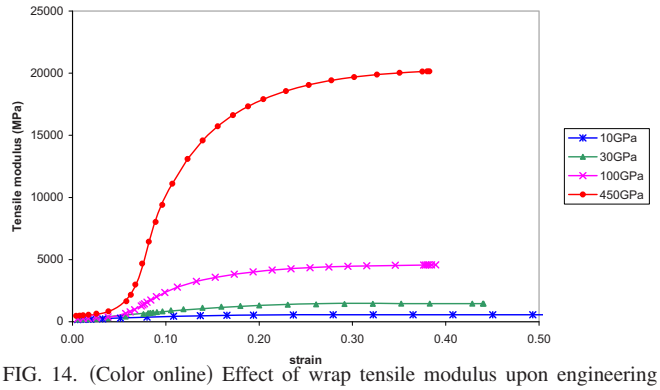

FIG. 14. (Color online) Effect of wrap tensile modulus upon engineering tensile modulus of yarn, wrap B, $\theta=20°$, component $\nu=0$, core E $=150$ MPa.

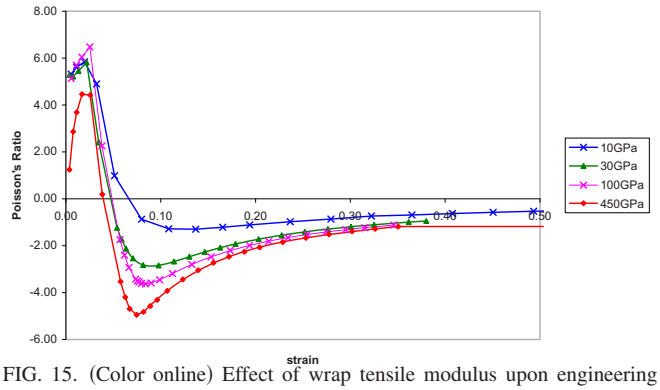

FIG. 15. (Color online) Effect of wrap tensile modulus upon engineering Poisson's ratio of yarn, wrap B, $\theta=20°$, component $\nu=0$, core E $=150$ MPa.

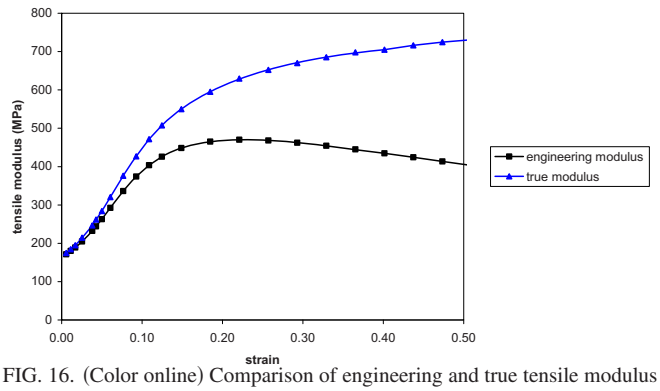

FIG. 16. (Color online) Comparison of engineering and true tensile modulus of yarn with wrap B, $\theta=20°$, component $\nu=0.45$.

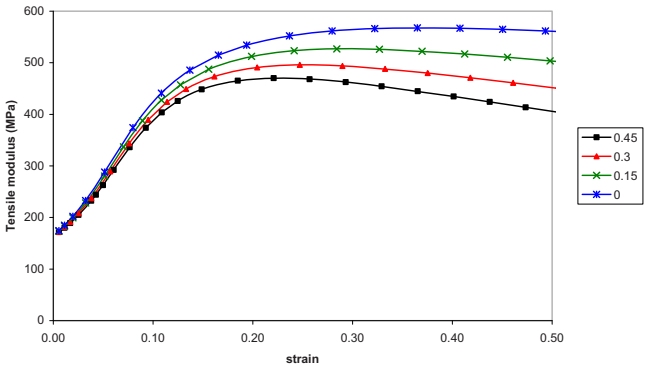

FIG. 17. (Color online) Effect of component Poisson's ratio upon engineering tensile modulus of yarn with wrap B, θ=20°. Both core and wrap are assigned the same value of ν in each case, ranging from 0 to 0.45.

self-supporting helix. The rate of change with respect to strain for the 20° case is much higher, so displacement of the core will begin at much lower strains.

D. Core/wrap tensile modulus ratio

Figures 14 and 15 show the effect of varying wrap modulus upon the tensile modulus and engineering Poisson's ratio [Eq. (5)] of the yarn, assuming component ν=0.

It is possible to effect a very high rate of change of yarn modulus with a suitable choice of component moduli. A higher wrap modulus gives a potentially higher negative yarn ν, with values here as low as −5. The nature of the yarn Poisson's ratio curve is discussed further in Sec. IV G.

E. Engineering versus true modulus

Thus far only the *engineering* tensile modulus has been considered, assuming that there is no change in cross-sectional area with strain. By measuring instantaneous cross-sectional area and calculating true strain as described in Sec. III we can also obtain the true tensile modulus. Figure 16 compares engineering and true tensile modulus as a function of longitudinal engineering strain for core and wrap components each having ν=0.45. The two moduli differ by 40% at 50% strain, indicating that consideration of cross-section changes for component ν=0.45 is essential.

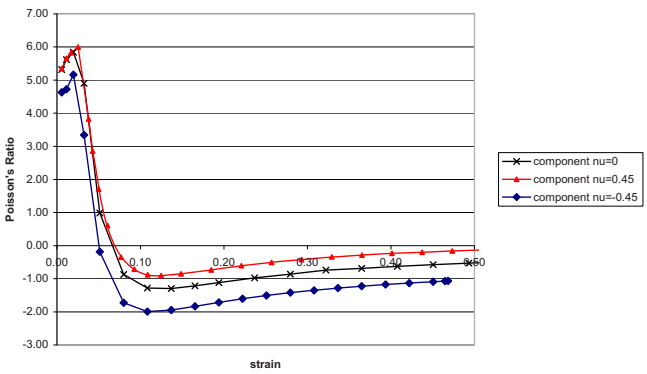

FIG. 18. (Color online) Effect of component Poisson's ratio upon engineering Poisson's ratio of yarn with wrap B, θ=20°.

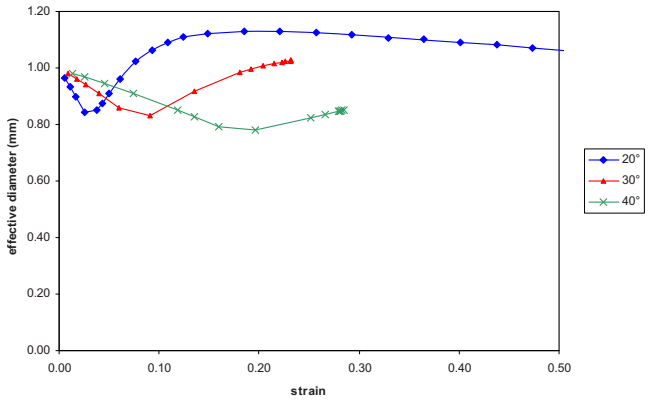

FIG. 19. (Color online) Effective diameter of yarn vs strain, wrap B, θ varying.

F. Component Poisson's ratios

Figure 17 shows the effect of varying the component Poisson's ratios upon yarn engineering tensile modulus (both core and wrap are assigned the same ν in each case). ν=0 shows an error of approximately 30% at 50% strain when compared to ν=0.45.

Auxetic monofilament fibers have been reported,[24] albeit at very low strains (typically below 2%). Figure 18 shows the Poisson's ratio of the *yarn* for negative, zero, and positive component ν, showing that increasing component ν reduces maximum negative Poisson's ratio; this will often be an issue of compromise in practical designs. Theoretically, use of auxetic components increases the maximum negative Poisson's ratio and reduces the high positive value at very low strains.

G. Poisson's ratio of the HAY

Figure 19 shows the variation in effective diameter with strain for the wrap B yarn with θ=20°, 30°, and 40°, and Figs. 20 and 21 the corresponding yarn engineering and true Poisson's ratios, respectively.

Referring to Fig. 20, at very low strains there is an initial phase of decrease in effective diameter corresponding to a positive ν. This is caused by reduction in wrap helix outer diameter while the core is displacing laterally and becoming helical but with an effective diameter as yet lower than that

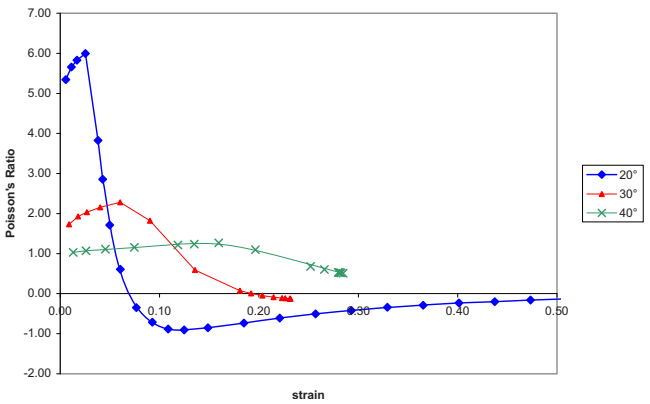

FIG. 20. (Color online) Engineering Poisson's ratio of yarn vs strain, wrap B, θ varying.

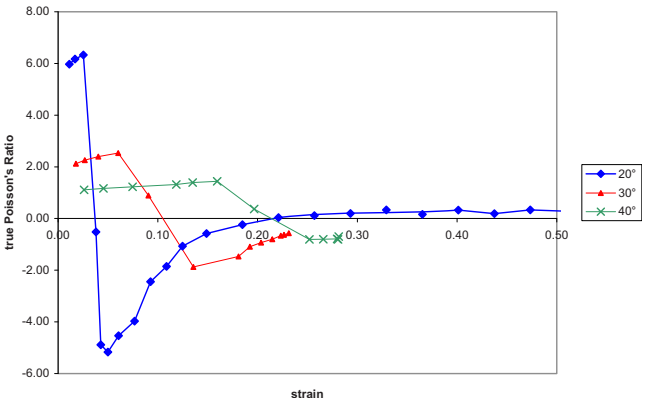

FIG. 21. (Color online) True Poisson's ratio of yarn vs strain, wrap B, θ varying.

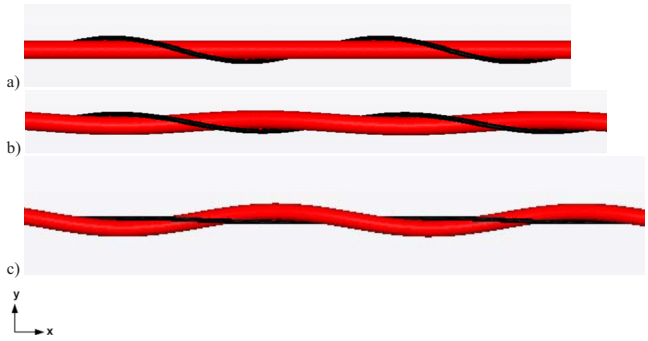

FIG. 22. (Color online) Yarn geometry (a) at zero strain; (b) at activation strain; and (c) above activation strain (auxetic).

of the wrap. At a specific strain value (for the $\theta=20°$ case, around 7% and for the $\theta=30°$ case, around 20%) the core helix may attain an outer diameter greater than D_{eo} [Fig. 22(c)] and then there is a zero-crossing of the Poisson's ratio. After this ν will become increasingly negative until the wrap helix inner diameter reaches zero (i.e., the wrap becomes cylindrical). From this point ν will tend back toward zero as the two components continue to reduce in cross-section. In the $\theta=40°$ case shown here there is no engineering auxetic effect although there is a true auxetic effect above about 22% strain (Fig. 21) and, as Fig. 11 illustrates, there is still an increase in tensile modulus at higher strains.

We define the strain at which the effective diameter exceeds its value at zero-strain as the *activation strain* of the yarn. Note that, depending upon ν of the components, it is also possible that the Poisson's ratio will never become negative (i.e., will not activate). It is the activation strain that is arguably of greatest practical interest. Initially the wrap does not undergo any [axial] strain: it is merely straightening and stresses in the wrap will be due exclusively to reaction forces from the core.

The initial positive ν cannot normally be avoided in practice except by pretensioning, if appropriate. Theoretically a HAY with an infinitesimal wrap and components with $\nu=0$ and infinite stiffness would not exhibit a positive ν. These are design pointers toward minimisation of the positive ν phase. In practice finite component stiffness can lead to embedding of the wrap in the core as strain increases: we shall discuss this in a forthcoming paper.

V. CONCLUSIONS

Generally, the behavior of HAYs may be divided into strain-dependent phases (Fig. 23): in region A the yarn has a positive ν; in region B true ν is negative but engineering ν remains positive; in region C both true ν and engineering ν are negative; in region D true ν becomes positive again while engineering ν remains negative.

HAYs with low wrap angles activate at lower strains. Higher wrap angles enable static performance to be opti-

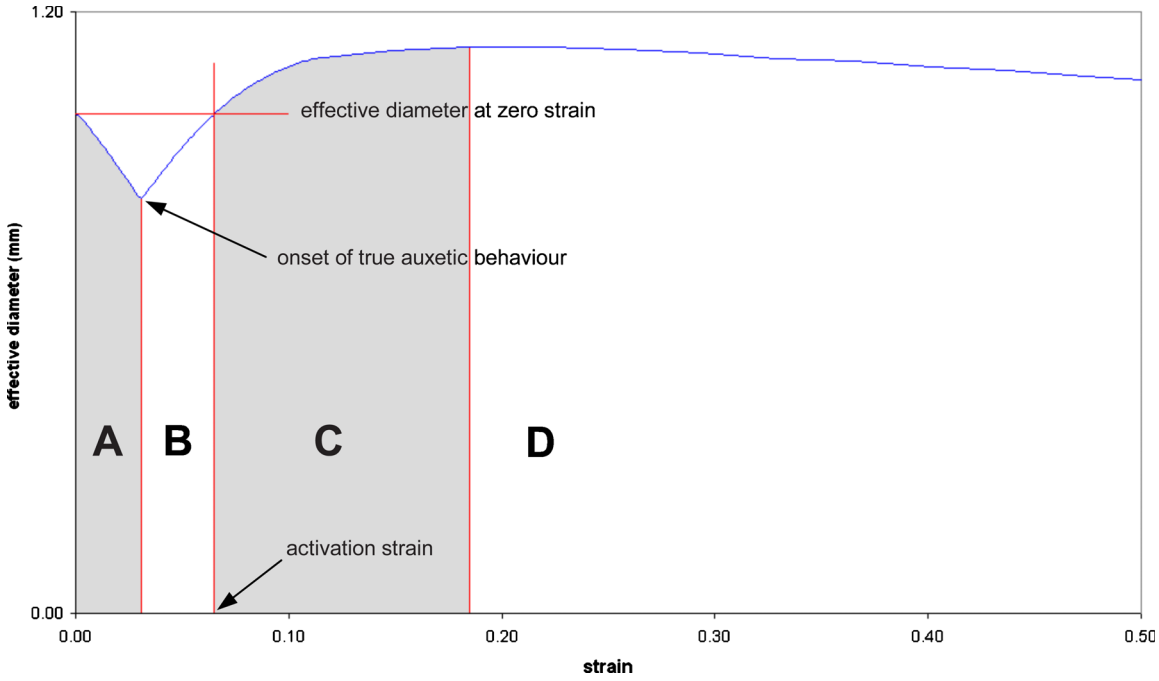

FIG. 23. (Color online) Strain-dependent behavior of the HAY.

mised for higher strains. To optimise auxetic behavior the wrap should ideally be of infinitesimal diameter while maintaining a relatively high stiffness, but in reality there will be practical limitations and cost implications in the use of very fine high modulus wraps.

Previous works have indicated that the tensile modulus of the wrap should be higher than that of the core[10–12] but we have shown that in choosing core and wrap materials the designer must consider the *stiffness* of these structures, i.e., the combination of diameter and modulus.

Although we have modeled the system assuming that the component fibers are comprised of linear isotropic materials, we observe that the component *structures* and HAYs exhibit nonlinear behavior due to nonzero component Poisson's ratios. Even at small strains, changes in cross-sectional area will cause a smooth deviation from linearity. It is important to note that in practical HAYs engineering tensile modulus is unreliable due to significant strain dependence of component cross-sectional areas. Therefore true tensile modulus should always be preferred.

Regarding model accuracy we have shown that a 10-cycle model is accurate within approximately 1.5% in avoiding errors due to end effects, and that a mesh density of approximately 10 000 elements/mm^3 or 10^{13} elements/m^3 is sufficient to model HAYs with core/wrap diameter ratios of around 5:1 and core/wrap tensile modulus ratios of around 1:60.

Most HAYs will have an initial positive Poisson's ratio behavior unless they are biased with a pretension, and there are practical limitations to maximum achievable negative Poisson's ratio due to finite positive Poisson's ratios in the components.

ACKNOWLEDGMENTS

This work is supported by the Engineering and Physical Sciences Research Council (Research Grant No. EP/F048394/1). The authors would like also to express their gratitude to Auxetix Ltd., Centre for the Protection of National Infrastructure, Heathcoat Fabrics Ltd., Home Office Scientific Development Branch and Monofil Trading Co. Ltd. for industrial and commercial support, and to their colleagues Mike Burns for technical support and Mike Felstead for configuring the SolidWorks parametric models.

[1] K. E. Evans, M. A. Nkansah, I. J. Hutchinson, and S. C. Rogers, Nature (London) **353**, 124 (1991).
[2] R. Lakes, Science **235**, 1038 (1987).
[3] N. Chan and K. E. Evans, J. Mater. Sci. **32**, 5945 (1997).
[4] I. G. Masters and K. E. Evans, Compos. Struct. **35**, 403 (1996).
[5] K. L. Alderson and K. E. Evans, Polymer **33**, 4435 (1992).
[6] C. Lees, J. F. V. Vincent, and J. E. Hillerton, Mater. Des. **1**, 19 (1991).
[7] J. N. Grima, R. Gatt, V. Zammit, J. J. Williams, K. E. Evans, A. Alderson, and R. I. Walton, J. Appl. Phys. **101**, 086102 (2007).
[8] D. J. Gunton and G. A. Saunders, J. Mater. Sci. **7**, 1061 (1972).
[9] P. B. Hook, "Auxetic Mechanisms, Structures & Materials," Ph.D. thesis, School of Engineering and Computer Science, University of Exeter, 2003.
[10] P. B. Hook, *Composite Fibre and Related Detection System*, WO2007125352, 2009.
[11] P. B. Hook, K. E. Evans, J. P. Hannington, C. Hartmann-Thompson, and T. R. Bunce, "Composite Materials and Structures," U.S. Patent No. US2007031667 (February 8, 2007).
[12] P. B. Hook, "Uses of Auxetic Fibres," U.S. Patent No. US2007210011 (September 13, 2007).
[13] W. Miller, P. B. Hook, C. W. Smith, X. Wang, and K. E. Evans, Compos. Sci. Technol. **69**, 651 (2009).
[14] M. R. Sloan, J. R. Wright, and K. E. Evans, "The Helical Auxetic Yarn–A novel structure for composites and textiles; Geometry, manufacture and mechanical properties," Mech. Mater. (to be published).
[15] R. B. Ramgulam and P. Potluri, *Progress in Industrial Mathematics at ECMI 2006* (Springer Berlin Heidelberg, 2008), pp.703–707.
[16] S. K. Batra, J. Text. Inst. **64**, 209 (1973).
[17] J. W. Phillips and G. A. Costello, Trans. ASME, J. Appl. Mech. **52**, 510 (1985).
[18] S. R. Ghoreishi, P. Davies, P. Cartraud, and T. Messager, Int. J. Solids Struct. **44**, 2943 (2007).
[19] J. W. S. Hearle and M. Konopasek, J. Appl. Polym. Sci.: Appl. Polym. Symp. **27**, 253 (1975).
[20] C. Lira, P. Innocenti, and F. Scarpa, Compos. Struct. **90**, 314 (2009).
[21] www.3ds.com
[22] www.solidworks.com
[23] http://rsbweb.nih.gov/ij/.
[24] K. L. Alderson, A. Alderson, P. J. Davies, G. Smart, N. Ravirala, and G. Simkins, J. Mater. Sci. **42**, 7991 (2007).